Aerospace Science and Technology ••• (••••) •••–•••

Contents lists available at SciVerse ScienceDirect

Aerospace Science and Technology

www.elsevier.com/locate/aescte

Modeling and control of a helicopter slung-load system

Tugrul Oktay *,[1], Cornel Sultan

Virginia Polytechnic Institute and State University, Blacksburg, VA, 24060, USA

ARTICLE INFO

Article history:
Received 10 February 2012
Received in revised form 22 March 2013
Accepted 27 March 2013
Available online xxxx

Keywords:
Variance constrained controllers
Helicopter slung-load operation
Stability robustness

ABSTRACT

This article investigates modeling and modern control for a helicopter and slung-load system. For this purpose complex, physics based, control oriented helicopter models are used. Point mass approach is used to model the external load's dynamics. The resulting nonlinear equations of motion are then trimmed for straight level flights and linearized around these flight conditions. Behaviors of representative trim variable values (i.e. cable angle and longitudinal and lateral cyclic blade pitch angles) and modes (i.e. flight dynamics and load modes) are thoroughly examined while some model parameters (e.g. cable length, load mass, and equivalent flat plate area) change. These behaviors are compared to data found in the literature. Furthermore, variance constrained controllers (i.e. output variance constrained and input variance constrained controllers) are applied for control system design. These controllers' performance is examined when they are aware of the slung-load's existence and when they are not aware of the slung-load.

1. Introduction

Carrying external loads has always been one of the important missions of both military and commercial helicopters. The dynamics of the overall system has received considerable attention since the 1960s. At the time there were two main reasons for this interest: the external load operations in the Vietnam war and the heavy-lift helicopter program (HLH). Interest in the load carrying ability of helicopters further grew due to the widespread use of helicopters in commercial and civil operations, which requires safe, rapid, and accurate deployment of heavy loads, eventually in hard to reach, confined spaces and in adverse conditions (e.g. fast emergy response in fire fighting, rescue missions in white out or brown out conditions, medical emergency responses, etc.).

Several theoretical studies to model the dynamics of helicopter slung-load systems were developed [24,12,13,37,10,8,16,43,38,44,7,9,45,14]. To the best of our knowledge the first theoretical study with slung-load carrying helicopter is described in [24]. For that study a simple three degrees of freedom model for slung-load dynamics was used and aerodynamic forces and moments acting on it were ignored. In Ref. [12] stability properties of a slung-load carrying helicopter with several feedback schemes were investigated. In the second part of the previous study reported in [13] suitable piloting strategies during different maneuvers were investigated. In all these studies [24,12,13] only hover and low speed flight conditions were investigated and the aerodynamic loads acting on the slung-load were neglected. In [37] stability of a slung-load carrying helicopter was studied considering aerodynamic forces acting on the external load. In that study using long cables, low weights and high speeds improved the stability of the external load. In Ref. [10] slung-load aerodynamics was also considered and via decreasing the drag force acting on the slung-load the stability properties were improved. We note that in order to gain rapid insight into the slung-load problem it was customary to tremendously simplify the load model. For example, in [8] the load was modeled as a point mass that behaves like a spherical pendulum suspended from a single point. However, recent works investigated more refined models. For example in Refs. [7,9,45,14] a thorough unsteady aerodynamics analysis was performed to model the slung-load carrying helicopter system.

Because of inherent helicopter flight instabilities, control design is vital for safe and performant helicopter operation. Therefore, control systems were involved in helicopter design from the early stages of both control and helicopter technology. Control design techniques for helicopters evolved throughout the years from classical pole placement methods [15,16,39] and simple feedback control approaches [2,1,21] to modern control methods based on linear matrix algebra like Linear Quadratic Regulator (LQR) and Linear Quadratic Gaussian (LQG) approaches [20,22,47,5], or H_∞ control synthesis [25,23,46]. Several control theory techniques (e.g. optimal control, adaptive control, feedback control) were applied for slung-load carrying helicopters [6,39,35,3,17,4]. For example, in [39] first some modes were redesigned to minimize pilot workload while maximizing the ability of the aircraft to maneuver predictably and precisely. Cable angle feedback was then used to improve stability of the helicopter slung-load system. Furthermore,

* Corresponding author.
E-mail address: tugruloktay52@gmail.com (T. Oktay).
[1] Currently Assistant Professor in Erciyes University.

1270-9638/$ – see front matter
http://dx.doi.org/10.1016/j.ast.2013.03.005

Nomenclature

p, q, r	Helicopter angular velocities ..... deg/s	$\theta_0, \theta_c, \theta_s$	Collective and two cyclic blade pitch angles ..... deg
u, v, w	Helicopter linear velocities ..... m/s	θ_{SL}, ϕ_{SL}	Slung-load orientation angles ..... deg
ϕ_A, θ_A, ψ_A	Helicopter Euler angles (roll, pitch, yaw) ..... deg	β_0	Collective blade flapping angle ..... deg
V_A	Flight speed of helicopter ..... knot	ζ_0	Collective blade lagging angle ..... deg

in [4] the operation of a helicopter in minimum time with slung-load through an environment with obstacles and with minimal slung-load oscillations was studied. For this system state and control trajectories were generated by formulating an optimal control problem.

In this article a different modern control strategy, namely variance constrained control [40–42,19,49,48] is applied to the helicopter slung-load system. Variance constrained control is an improved LQG strategy because it guarantees satisfaction of constraints expressed using the output or the input variances. By using variances, the control design process effectively manipulates second-order information which is very advantageous because tractable solutions to quadratic optimal constrained control problems are possible [40,41]. In control theory it is generally preferred to use second-order information because it permits parameterization of controllers in terms of physically meaningful data, for example the state covariance matrix. Moreover, for strongly coupled large multi-input and multi-output (MIMO) systems, like the ones encountered in helicopter control, such methods offer guarantees on the transient behavior of individual parameters by imposing upper bounds on the variance of these variables.

The article presents first the development of the control oriented helicopter model used in this work. Some trim and modal data are given for Puma SA 330 to illustrate how this model captures the dynamics of realistic helicopters. Then trim and linearization is performed for the helicopter slung-load model. Behaviors of representative trim variable values such as longitudinal cable angle and longitudinal and lateral cyclic blade pitch angles as well as eigenvalues corresponding to fuselage (i.e. flight dynamics) and load modes are examined while some model parameters (e.g. cable length, load mass, and equivalent flat plate area) change. These behaviors are compared to data found in the literature, pointing out similarities and differences. Lastly, output variance constrained and input variance constrained controllers are designed using linearized models of unloaded as well as slung-load carrying helicopters. The performance of these controllers is examined when they are used for the system they are designed for, i.e. when they are "aware" of the slung-load's existence, and when they are not aware of the slung-load. Based on these studies recommendations regarding the implementation of such controllers are made.

2. Helicopter model

The modeling process used to develop the helicopter model employed in this article was presented in [28] (for more details the reader may consult [26]). In summary, this process involves application of physics principles, directly leading to dynamic models composed of finite sets of ordinary differential equations (ODEs). This is very useful for control system design since it makes the direct use of modern control theory easy. This is so because modern control design relies on state space representations of the system's dynamics, which are readily obtained from ODEs. The models obtained using the method summarized above capture both fuselage and blade (i.e. flapping and lead-lagging, in some cases even blade flexibility [28]) dynamics. These models consist of nonlinear ODEs, but because they have too many terms their use in fast computation is impossible. Therefore, a systematic model simplification method which does not alter the type or number of equations was applied to reduce the number of terms in the nonlinear ODEs. This method, which is popular in the helicopter literature, is called "ordering scheme" and it amounts to eliminating terms that have small magnitude with respect to dominant terms (see [28,26] for more details).

The helicopter model obtained using the philosophy described above includes fuselage, empennage (i.e. tail rotor hub and shaft, and horizontal tailplane), landing gear, fully articulated main rotor (i.e. with 4 blades and blade flapping and lagging hinges), and main rotor downwash [28]. As a consequence, the model is fairly complex with a total of 28 nonlinear equations: 9 fuselage equations, 8 blade flapping equations, 8 blade lead-lagging equations, 3 main rotor downwash equations. These nonlinear equations were solved for trim conditions. In this article trim is defined as finding the controls and state variables to achieve straight level flight with constant speed (V_A). After inserting the trim conditions for these nominal flights into the dynamic nonlinear system of 28 differential equations, 17 trim equations (i.e. $0 = 0$ equations are eliminated) with 17 unknowns were obtained. The trim values of helicopter angular velocities (p, q, r) and yaw angle (ψ_A) are zero. The trim values of helicopter linear velocities were easily expressed using well known formulas [28] in terms of flight speed (V_A), roll (ϕ_A) and pitch (θ_A) angles of helicopter. These trim equations were solved using Matlab for different straight level flight conditions.

After trimming, the model was linearized using Maple, yielding continuous linear time-invariant (LTI) systems

$$\dot{x}_p = A_p x_p + B_p u \tag{1}$$

where x_p and u are the perturbed states and controls. Matrices A_p and B_p are of size 25×25 and 25×4. Puma SA 330 helicopter (see [36]) was used to validate the models used in our work. The 25 states are 9 fuselage states, 8 blade flapping states, and 8 blade lead-lagging states, while the four controls are 3 main rotor (collective, θ_0, lateral cyclic, θ_c, and longitudinal cyclic, θ_s, blade pitch angles) and 1 tail rotor (collective) control input.

To validate our helicopter model we compared trim values as well as linearized dynamics data with data found in the literature. In general these comparisons showed very good agreement with existing data. For example, Table 1 presents the eigenvalues of the flight dynamics modes for three straight level flight conditions obtained using our model and the data in Ref. [36] for Puma SA 330. Fig. 1 shows flapping and lead-lagging eigenvalues which were found qualitatively similar to data reported in the literature (e.g. Ref. [36]). The corresponding values of the trim states are given in Eqs. (2a)–(2c). All trim results show good correspondence with data in the literature (see Refs. [28,26]). Also see Refs. [27,29–34] for other control applications of our helicopter models developed and validated using this strategy.

$$_{hover}x_0 = [\underbrace{0.2696, 0.0315, -0.0377, 0.4522}_{\theta_{0_0}, \theta_{c_0}, \theta_{s_0}, \theta_{T_0}}, \underbrace{-0.0470, 0.0170}_{\phi_{A_0}, \theta_{A_0}},$$
$$\underbrace{0.0882,\ 0.0378, 0.0312, 0}_{\beta_{0_0}, \beta_{c_0}, \beta_{s_0}, \beta_{d_0}},$$

Please cite this article in press as: T. Oktay, C. Sultan, Modeling and control of a helicopter slung-load system, Aerospace Science and Technology (2013), http://dx.doi.org/10.1016/j.ast.2013.03.005

Table 1
Comparison of flight dynamics modes.

Mode (rad/s)	Hover		$V_A = 40$ kts		$V_A = 80$ kts	
	Ref. [36]	Our modes	Ref. [36]	Our modes	Ref. [36]	Our modes
1st (Dutch Roll)	$0.2772 \pm 0.5008i$	$0.2215 \pm 0.5966i$	$-0.1543 \pm 0.9181i$	$-0.0434 \pm 1.0846i$	$-0.1854 \pm 1.0546i$	-0.1736 ± 2.0642
2nd (Phugoid)	$-0.0410 \pm 0.5691i$	$0.0587 \pm 0.3589i$	$0.0275 \pm 0.3185i$	$-0.0143 \pm 0.3253i$	$-0.0085 \pm 0.2074i$	$-0.0138 \pm 0.1674i$
3rd (Yaw subsidence)	-0.2697	-0.1449	-0.0976	-0.0703	-0.1358	-0.04786
4th (Roll subsidence)	-0.3262	-1.1944	-0.9817	-0.7140	-1.5163	-0.7587
5th (Roll-pitch oscillation)	$-1.2990 \pm 0.2020i$	$-0.6536 \pm 0.3536i$	$-1.0394 \pm 0.2798i$	$-0.6125 \pm 1.1300i$	$-0.9252 \pm 1.0503i$	-0.6759 ± 1.8865

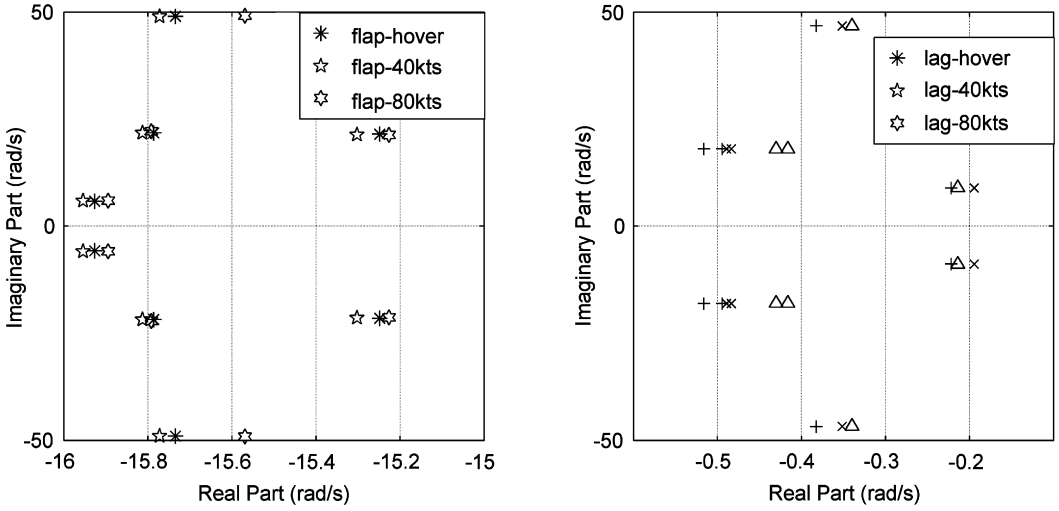

Fig. 1. Helicopter blade flapping and lead-lagging modes.

$$\underbrace{0.0203, 0.0042, -0.0059, 0,}_{\zeta_{0_0}, \zeta_{c_0}, \zeta_{s_0}, \zeta_{d_0}}$$
$$\underbrace{0.0437, 11.7439, 0.5263]^T}_{\chi_0, \lambda_{0_0}, \lambda_{c_0}} \quad (2a)$$

$$_{40kts}x_0 = [\underbrace{0.2753, 0.0370, -0.0908, 0.4857}_{\theta_{0_0}, \theta_{c_0}, \theta_{s_0}, \theta_{T_0}}, \underbrace{-0.0456, 0.0272}_{\phi_{A_0}, \theta_{A_0}},$$
$$\underbrace{0.0795, 0.0592, 0.0252, 0}_{\beta_{0_0}, \beta_{c_0}, \beta_{s_0}, \beta_{d_0}},$$
$$\underbrace{0.0218, 0.0010, -0.0082, 0}_{\zeta_{0_0}, \zeta_{c_0}, \zeta_{s_0}, \zeta_{d_0}},$$
$$\underbrace{1.2523, 6.2236, 9.2217]^T}_{\chi_0, \lambda_{0_0}, \lambda_{c_0}} \quad (2b)$$

$$_{80kts}x_0 = [\underbrace{0.2468, 0.0319, -0.1017, 0.3626}_{\theta_{0_0}, \theta_{c_0}, \theta_{s_0}, \theta_{T_0}}, \underbrace{-0.0255, 0.0110}_{\phi_{A_0}, \theta_{A_0}},$$
$$\underbrace{0.0748, 0.0463, 0.0102, 0}_{\beta_{0_0}, \beta_{c_0}, \beta_{s_0}, \beta_{d_0}},$$
$$\underbrace{0.0159, -0.0028, -0.0071, 0}_{\zeta_{0_0}, \zeta_{c_0}, \zeta_{s_0}, \zeta_{d_0}},$$
$$\underbrace{1.4825, 3.1898, 5.9822]^T}_{\chi_0, \lambda_{0_0}, \lambda_{c_0}} \quad (2c)$$

where all the trim angles are in radians and downwash terms (i.e. $\lambda_{0_0}, \lambda_{c_0}$) are in m/s.

3. Slung-load modeling

The derivation of the governing equations of motion for the external load follows [8,16,43,38,44], using the next set of assumptions. The external load is modeled as a point mass. The atmosphere is stationary and a quasi-steady drag force acts in the direction of the local airflow. The external load is not affected by the main rotor and tail rotor inflow. The cable is inelastic and massless and there is no aerodynamic force acting on the cable.

A helicopter slung-load system with all the required reference frames is illustrated in Fig. 2 where M is the external load mass and l is the cable length. The unit vectors of the hook frame $(\hat{x}_H, \hat{y}_H, \hat{z}_H)$ are always parallel to those of the gravity frame. The position of the external load is defined by two angles, θ_{SL} and ϕ_{SL}, where θ_{SL} is the angle between $\hat{z}_H$ and the cable, and ϕ_{SL} is the azimuth angle of the load. The position vector of the load with respect to (w.r.t.) helicopter cg, $\vec{R}$, is

$$\vec{R} = \vec{R}_H + \vec{R}_L \quad (3)$$

Here $\vec{R}_H$ is the position vector of the load w.r.t. the hook point and in hook frame it is

$$\vec{R}_L = -l \sin(\theta_{SL}) \cos(\phi_{SL}) \hat{x}_H + \sin(\theta_{SL}) \sin(\phi_{SL}) \hat{y}_H + \cos(\theta_{SL}) \hat{z}_H \quad (4)$$

while $\vec{R}_L$ is the position vector of the hook point w.r.t. the helicopter's center of gravity (cg) and in aircraft frame (whose unit vectors are $\hat{x}_A, \hat{y}_A, \hat{z}_A$) it is

$$\vec{R}_H = x_S \hat{x}_A + y_S \hat{y}_A + z_S \hat{z}_A \quad (5)$$

The absolute velocity vector of the load w.r.t. the inertial frame is

Please cite this article in press as: T. Oktay, C. Sultan, Modeling and control of a helicopter slung-load system, Aerospace Science and Technology (2013), http://dx.doi.org/10.1016/j.ast.2013.03.005

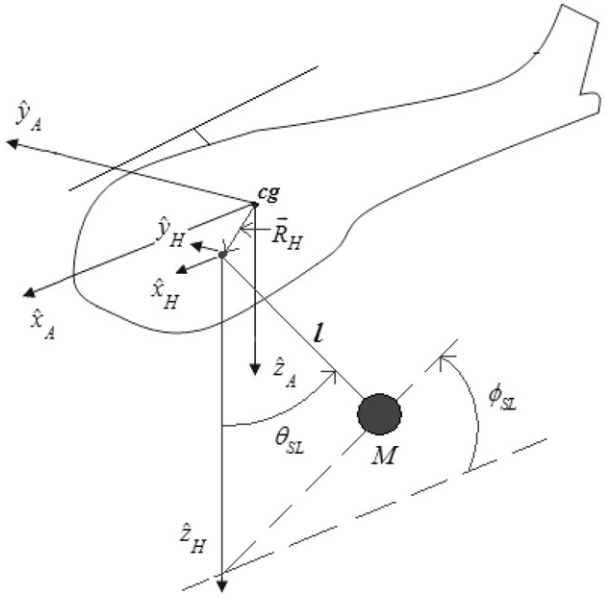

Fig. 2. Helicopter slung-load system.

$$\vec{V} = \vec{V}_A + \vec{\omega}_A \otimes \vec{R} \tag{6}$$

where $\otimes$ denotes the vector cross product, $\vec{V}_A$ is the absolute velocity of the helicopter w.r.t. the inertial frame, $\vec{\omega}_A$ is the angular velocity of the helicopter w.r.t. the inertial frame. In aircraft frame they are

$$\vec{V}_A = u\hat{x}_A + v\hat{y}_A + w\hat{z}_A, \qquad \vec{\omega}_A = p\hat{x}_A + q\hat{y}_A + r\hat{z}_A \tag{7}$$

The absolute acceleration vector of the load w.r.t. the inertial frame is

$$\vec{a} = \vec{a}_A + \dot{\vec{\omega}}_A \otimes \vec{R} + \vec{\omega}_A \otimes (\vec{\omega}_A \otimes \vec{R}) \tag{8}$$

where $\vec{a}_A$ is the absolute acceleration of the helicopter w.r.t. the inertial frame. The drag force vector acting on the load is

$$\vec{D} = \frac{1}{2}\rho|\vec{V}|\vec{V}S \tag{9}$$

where S is the equivalent flat plate area (which includes the drag coefficient of the external load). The governing equations of the slung-load's motion were derived by summing up inertial, aerodynamic, and gravitational moments around the suspension point.

$$\vec{R}_L \otimes (-M\vec{a} + M\vec{g} + \vec{D}) = 0 \tag{10}$$

where $\vec{g}$ is the gravitational acceleration vector.

When this approach is used to model the slung-load 4 additional nonlinear ODEs are generated which describe the load motion. Thus, at the end of the entire modeling process we obtain a total of 32 nonlinear ODEs which describe the dynamics of the helicopter slung-load system.

4. Trim and linearization

Recall that in this article trim is defined as the condition for which straight level flight with constant speed is achieved. Compared to the unloaded helicopter (i.e. helicopter without a slung-load), there are 2 additional trim equations and 2 additional trim unknowns for the slung-load (i.e. slung-load angles). Trimming for this system was performed similarly with trimming of the unloaded helicopter, i.e. by using Matlab's *fsolve* procedure. The results thus found were verified by inserting them into the nonlinear dynamic equations of motion of the helicopter slung-load system. Very small numbers (around 10^{-10}) were found which proves that our trimming procedure is correct. In Eqs. (11a)–(11c) we give the trim values for three flight conditions (hover and straight level flight at 40 and 80 kts), for $M = 500$ kg, $l = 5$ m, $S = 0.4$ m^2 whereas in Fig. 3 we give the variation of the trim value of the angle θ_{SL} with the straight level flight speed, V_A (note that for straight level flight the trim value of ϕ_{SL} is always zero). We remark that the addition of a load to the unloaded helicopter leads to minor changes in the values of the trim parameters (see Eqs. (2a)–(2c)). This is a very important observation because it indicates that the trim conditions are robust with respect to load addition, which is, of course, a desirable feature. Essentially, it is one of the crucial requirements that a particular helicopter should meet in order to be used in load carrying operations.

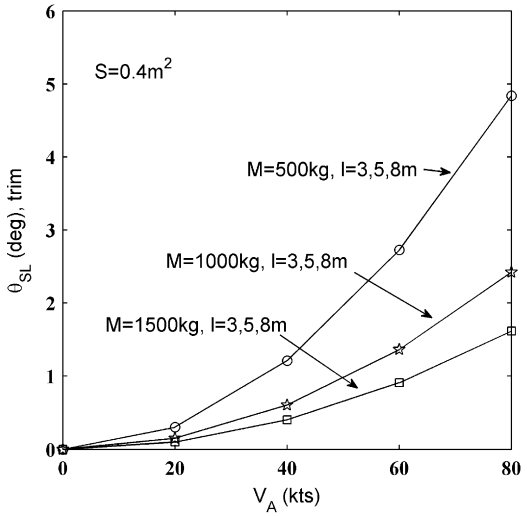

Fig. 3. Variation of longitudinal slung-load trim angle with flight speed (V_A).

After trimming, the helicopter slung-load system was linearized using Maple considering $M = 500$ kg, $l = 5$ m, $S = 0.4$ m^2 where S is the equivalent surface area of the load (see Appendix A, Table A.1 for numerical values of key helicopter parameters; additional data can be found in Ref. [26]). Linearization resulted in continuous LTI systems. Compared to the unloaded helicopter there are 4 additional load states for the helicopter slung-load system, i.e. longitudinal and lateral load angles, θ_{SL} and ϕ_{SL}, respectively, and their time derivatives, $\dot{\theta}_{SL}$ and $\dot{\phi}_{SL}$. For this system, Eq. (1), which is the generic LTI system equation, applies with matrices A_p and B_p of size 29×29 and 29×4.

$$\begin{aligned} {}_{S\_hover}x_0 = [&\underbrace{0.2795, 0.0356, -0.0361, 0.4979}_{\theta_{0_0}, \theta_{c_0}, \theta_{s_0}, \theta_{T_0}}, \\ &\underbrace{-0.0458, 0.0159}_{\phi_{A_0}, \theta_{A_0}}, \underbrace{0.0959,\ 0.0361, 0.0356, 0}_{\beta_{0_0}, \beta_{c_0}, \beta_{s_0}, \beta_{d_0}}, \\ &\underbrace{0.0224, 0.0053, -0.0062, 0}_{\zeta_{0_0}, \zeta_{c_0}, \zeta_{s_0}, \zeta_{d_0}}, \\ &\underbrace{0.0420, 12.2398, 0.5264}_{\chi_0, \lambda_{0_0}, \lambda_{c_0}}]^T \end{aligned} \tag{11a}$$

$$\begin{aligned} {}_{S\_40kts}x_0 = [&\underbrace{0.2878, 0.0428, -0.0918, 0.5482}_{\theta_{0_0}, \theta_{c_0}, \theta_{s_0}, \theta_{T_0}}, \\ &\underbrace{-0.0458, 0.0256}_{\phi_{A_0}, \theta_{A_0}}, \underbrace{0.0871,\ 0.0577, 0.0301, 0}_{\beta_{0_0}, \beta_{c_0}, \beta_{s_0}, \beta_{d_0}}, \\ &\underbrace{0.0246, 0.0017,\ -0.0086, 0}_{\zeta_{0_0}, \zeta_{c_0}, \zeta_{s_0}, \zeta_{d_0}} \end{aligned}$$

Please cite this article in press as: T. Oktay, C. Sultan, Modeling and control of a helicopter slung-load system, Aerospace Science and Technology (2013), http://dx.doi.org/10.1016/j.ast.2013.03.005

$$\underbrace{1.2321, 6.7215, 9.7495}_{\chi_0,\lambda_{0_0},\lambda_{c_0}}]^T \tag{11b}$$

$$x_{S\_80kts} = [\underbrace{0.2590, 0.0365,}_{\theta_{0_0},\theta_{c_0},\theta_{s_0},\theta_{T_0}} \underbrace{-0.1043, 0.4103}, \underbrace{-0.0258, 0.0058}_{\phi_{A_0},\theta_{A_0}}, \underbrace{0.0821, 0.0441, 0.0128, 0}_{\beta_{0_0},\beta_{c_0},\beta_{s_0},\beta_{d_0}}, \underbrace{0.0181, 0.0029, -0.0071, 0}_{\zeta_{0_0},\zeta_{c_0},\zeta_{s_0},\zeta_{d_0}}, \underbrace{1.4811, 3.4633, 6.4863}_{\chi_0,\lambda_{0_0},\lambda_{c_0}}]^T \tag{11c}$$

where all the trim angles are in radians and downwash terms (i.e. $\lambda_{0_0}, \lambda_{c_0}$) are in m/s.

5. Variance constrained controllers

Helicopters are always exposed to output and input limitations and a key requirement is minimization of control energy. These requirements are even more stringent for helicopters carrying loads via a slung-load system. For example large deviations of the helicopter slung-load system from the trim position cannot be tolerated for safety reasons and for stability of the aggregate system. Furthermore, control energy is generated by on board batteries or via fuel consumption, in which case energy minimization is equivalent to fuel consumption minimization. In either case, minimization of control energy leads to mass reduction of the entire system, which is always a desirable objective for airborne systems. For these reasons, in this article modern output variance constrained control (OVC) and input variance constrained control (IVC) (see Refs. [40–42,19,49,48] for more details) are studied for helicopter slung-load control system design. These controllers guarantee satisfaction of output (OVC) or input (IVC) constraints while also reducing the control energy.

The OVC idea is summarized next for completeness of the article. For a given continuous LTI system which is stabilizable and detectable

$$\dot{x}_p = A_p x_p + B_p u + w_p, \qquad y = C_p x_p, \qquad z = M_p x_p + v \tag{12}$$

and a positive definite input penalty matrix, $R > 0$, find a full order dynamic controller

$$\dot{x}_c = A_c x_c + F z, \qquad u = G x_c \tag{13}$$

to minimize the control energy, i.e.

$$\min_{A_c,F,G} E_\infty u^T R u \tag{14}$$

subject to variance constraints on the output, i.e.

$$E_\infty y_i^2 \leqslant \sigma_i^2, \quad i = 1, \ldots, n_y \tag{15}$$

where z represents sensor measurements, w_p and v are zero-mean uncorrelated Gaussian white noises with intensities W and V respectively, σ_i^2 is the upper bound imposed on the i-th output variance, and n_y is the number of outputs. OVC solution reduces to a linear quadratic Gaussian (LQG) problem by choosing the output penalty matrix, $Q > 0$, function of the inequality constraints on output variances. An algorithm for the selection of Q is presented in [19,49] and used herein. After converging on Q, OVC parameters are

$$A_c = A_p + B_p G - F M_p, \qquad F = X M_p^T V^{-1}, \qquad G = -R^{-1} B_p^T K \tag{16}$$

where X and K are solutions of two algebraic Riccati equations:

$$0 = X A_p^T + A_p X - X M_p^T V^{-1} M_p X + W \tag{17a}$$

$$0 = K A_p + A_p^T K - K B_p R^{-1} B_p^T K + C_p^T Q C_p \tag{17b}$$

The IVC problem is basically the dual of OVC: for a given continuous LTI, stabilizable and detectable system (Eq. (12)) and a given positive definite output penalty matrix, $Q > 0$, a full order dynamic controller (Eq. (12)) must be found to solve

$$\min_{A_c,F,G} E_\infty y^T Q y \tag{18}$$

subject to

$$E_\infty u_i^2 \leqslant \mu_i^2, \quad i = 1, \ldots, n_u \tag{19}$$

where μ_i^2 is the upper bound variance imposed on the i-th input, and n_u is the number of inputs. Note that whereas OVC explicitly minimizes control energy, IVC reduces this energy via the inequality constraints on input variances. IVC solution reduces to a LQG problem solution by choosing a positive definite input penalty matrix, $R > 0$. An algorithm for the selection of R is also presented in [49]. After converging on R, IVC is obtained using Eq. (16). Compared to LQG, OVC and IVC provide an intelligent way of choosing Q and R, which guarantees satisfaction of constraints.

6. Trim and stability results

6.1. Validation of helicopter slung-load system trims

As already mentioned we first conducted validation studies for the helicopter model, which led to the conclusion that our model captures both the trim conditions and the essential dynamics of the unloaded helicopter accurately (see Section 2). In addition, we also conducted numerous numerical experiments for the helicopter slung-load system in order to validate the entire system. Some trim results for this system were reported in Eqs. (11a)–(11c). The first important conclusion is that our helicopter trim values are in the range reported in the literature (see Refs. [8,16,43,38,44,26] for details and discussions). As already emphasized, these values do not differ substantially from the values for the unloaded helicopter (i.e. the helicopter is robust, as far as trim concerns, with respect to load addition). We then focused our attention on validating the results for the load trim angles, as discussed next.

We extensively studied the variation of the longitudinal load trim angle with key parameters, such as the mass of the load and the trim flight speed, V_A, or advance ratio, μ, ascertaining good agreement with data reported in the literature. For example, when the external load mass decreases, for a fixed flight speed the trim value of the cable angle, θ_{SL}, becomes greater, and when the forward flight speed increases, for a fixed mass, this angle increases with the flight speed, as showed in Fig. 3. This behavior is similar to the one reported in [38] and expected from a force balance analysis. The cable length does not affect the trim value of the cable angle, which is also similar with the observations reported in [16] (see Fig. 3) and expected. Also, similarly with results reported in [16], the value of the trim lateral cyclic blade pitch angle, θ_c, increases when load mass increases for any flight speed between hover to 80 kts, or equivalently for advance ratios between 0 and 0.4, as showed in Fig. 4. The variation of this quantity with the advance ratio (or flight speed) is as well analogous to the variation reported in Ref. [16]. Moreover, the value of the trim longitudinal cyclic blade pitch angle, θ_s, increases for low advance ratios (flight speeds) when the load mass, M, increases, which agrees with results reported in [16] (see Fig. 5). On the other hand, this quantity decreases for higher flight speeds (i.e. above 20 kts, which

Please cite this article in press as: T. Oktay, C. Sultan, Modeling and control of a helicopter slung-load system, Aerospace Science and Technology (2013), http://dx.doi.org/10.1016/j.ast.2013.03.005

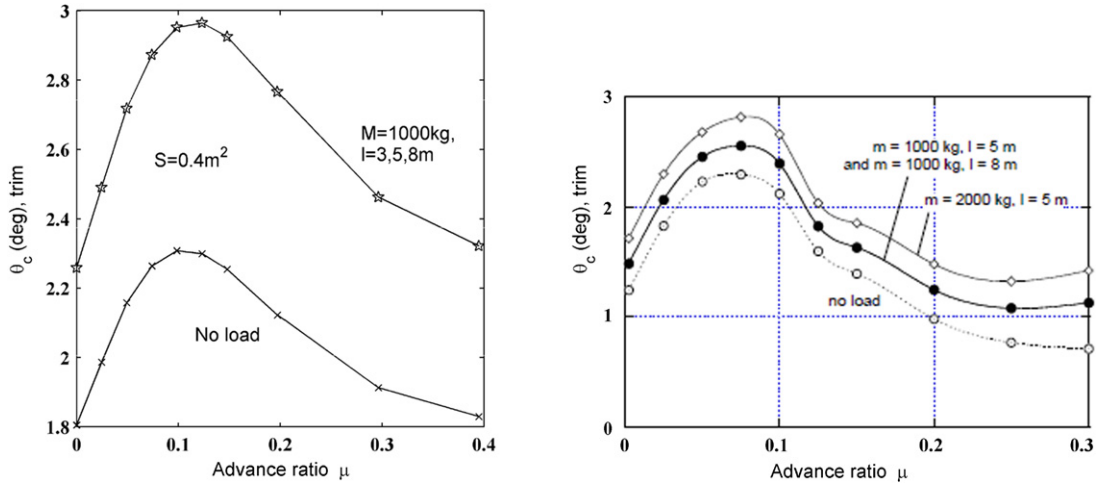

Fig. 4. Variation of trim lateral cyclic blade pitch angle with advance ratio (left: our results; right: results reproduced from Ref. [16]; note: $\mu = \frac{V_A \cos(\alpha_F)}{\Omega R}$, $\Omega R = 220.98$ m/s for UH-60, α_F: fuselage angle of attack).

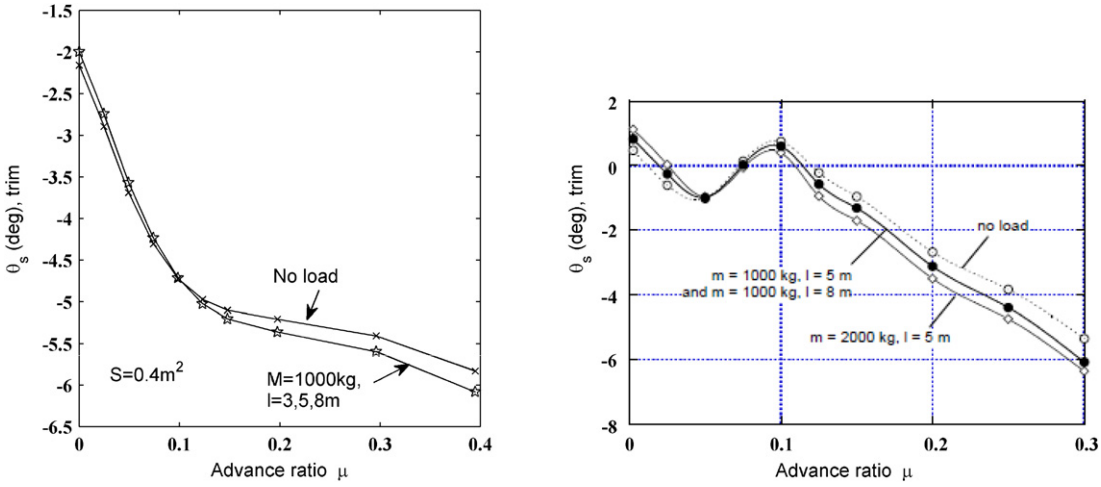

Fig. 5. Variation of trim longitudinal cyclic blade pitch angle with advance ratio (left: our results; right: results reproduced from Ref. [16]).

approximately corresponds to an advance ratio of 0.1) when the load mass, M, increases, which also agrees with results reported in [16] (see Fig. 5). Furthermore, both trim values of θ_c and θ_s are not affected by cable length (see Figs. 3 and 4). The only discrepancy between our results and those reported in Ref. [16] is noticed in Fig. 5, for a small range of advance ratios (between 0.05 and 0.1), when the variation of the value of the trim longitudinal cyclic blade pitch angle, θ_s, with the advance ratio (and flight speed) is reversed compared to our results. This local discrepancy can be explained by inherent differences between the modeling procedure used here and the one used in Ref. [16] and by the helicopter data themselves (i.e. Puma SA 330 for our model and Sikorsky UH-60 for Ref. [16]). However, the overall conclusion that good agreement was obtained is not substantially affected by this difference.

6.2. Validation of helicopter slung-load system poles

When control design is pursued it is important to make sure that the open loop dynamics of the system to be controlled is correctly captured by the model used in control design. For this purpose we proceeded to validating: a) the flight dynamics modes; b) the blade modes (flapping, lead-lagging modes); c) the load modes because the subject of this article is the control of the entire helicopter slung-load system. Validation of flight dynamics and blade modes via eigenvalues comparison with data available in the literature has been extensively studied and reported in our previous works for unloaded helicopters (e.g. Refs. [28,26] and [30]) for numerous flight conditions, with or without blade flexibility modeled. We also reported some of these validation data relevant to the flight cases considered in this article in Table 1 and Fig. 1. In the following, we focus on the novel aspects relevant to this article, namely validation of the load modes. We note that our extensive literature search revealed that very few papers report on the poles (i.e. eigenvalues) of helicopter slung-load systems. No published data has been found for Puma SA 330 but some papers report a number of poles for UH-60. Therefore, this article is probably the first one that reports on the poles of the helicopter slung-load system for Puma SA 330. We compare these results with the ones found in the literature for UH-60, but, of course, since the helicopters are different, discrepancies are expected to occur. These discrepancies are pointed out in the following discussion.

For poles validation we performed the following analysis. We first linearized the helicopter slung-load model for hover, $S = 0.4$ m^2, $l = 5$ m, and different load masses, of 500, 1000, and 1500 kg. For all these scenarios we computed the eigenvalues of the open loop matrix (i.e. matrix A_p of size 29×29). The first key observation is that the load modes have larger variations than the Dutch Roll and Phugoid modes when the load mass changes. This agrees with results reported in Ref. [10] (also see Fig. 6 reproduced from Ref. [16]). Second, the load modes display

Please cite this article in press as: T. Oktay, C. Sultan, Modeling and control of a helicopter slung-load system, Aerospace Science and Technology (2013), http://dx.doi.org/10.1016/j.ast.2013.03.005

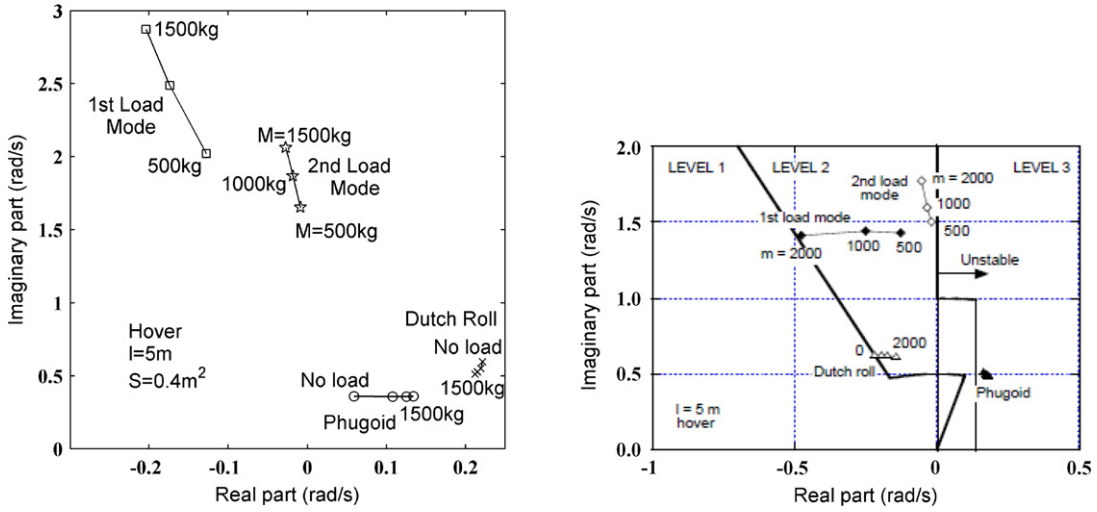

Fig. 6. Variation of some helicopter and slung-load modes with load mass (left: our results; right: results reproduced from Ref. [16]).

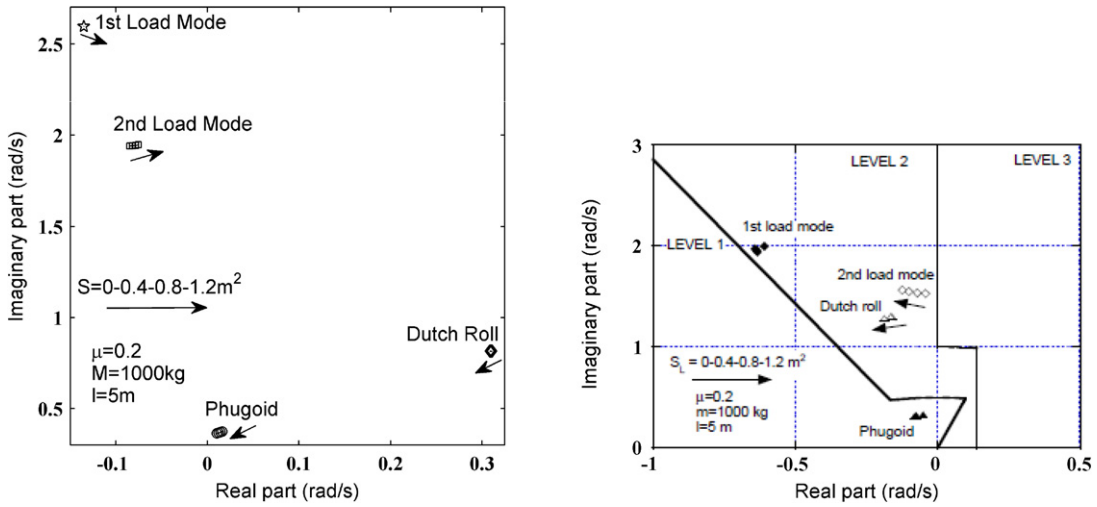

Fig. 7. Variation of some helicopter and slung-load modes with equivalent flat plate area (left: our results; right: results reproduced from Ref. [16]).

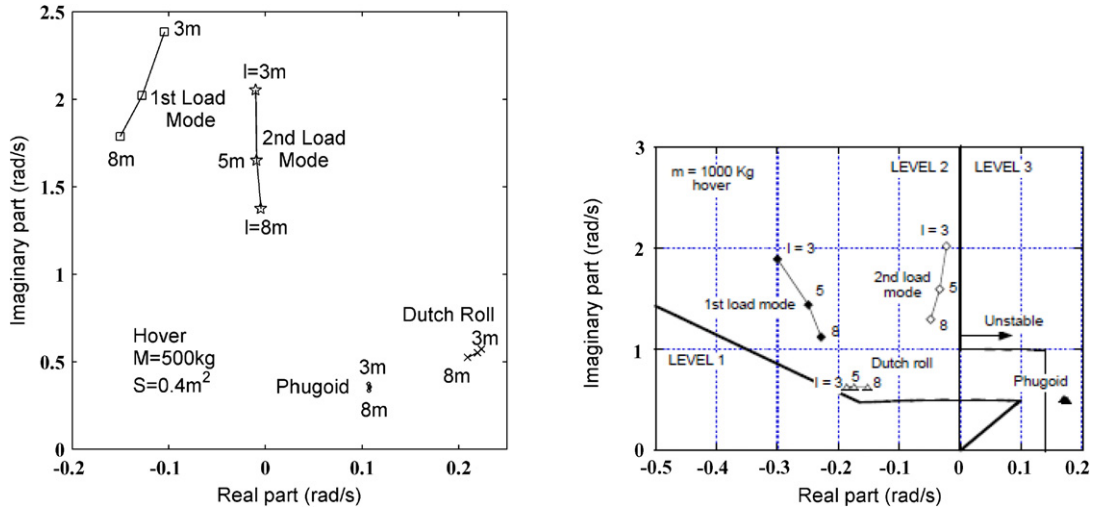

Fig. 8. Variation of some helicopter and slung-load modes with cable Length (left: our results; right: results reproduced from Ref. [16]).

Please cite this article in press as: T. Oktay, C. Sultan, Modeling and control of a helicopter slung-load system, Aerospace Science and Technology (2013), http://dx.doi.org/10.1016/j.ast.2013.03.005

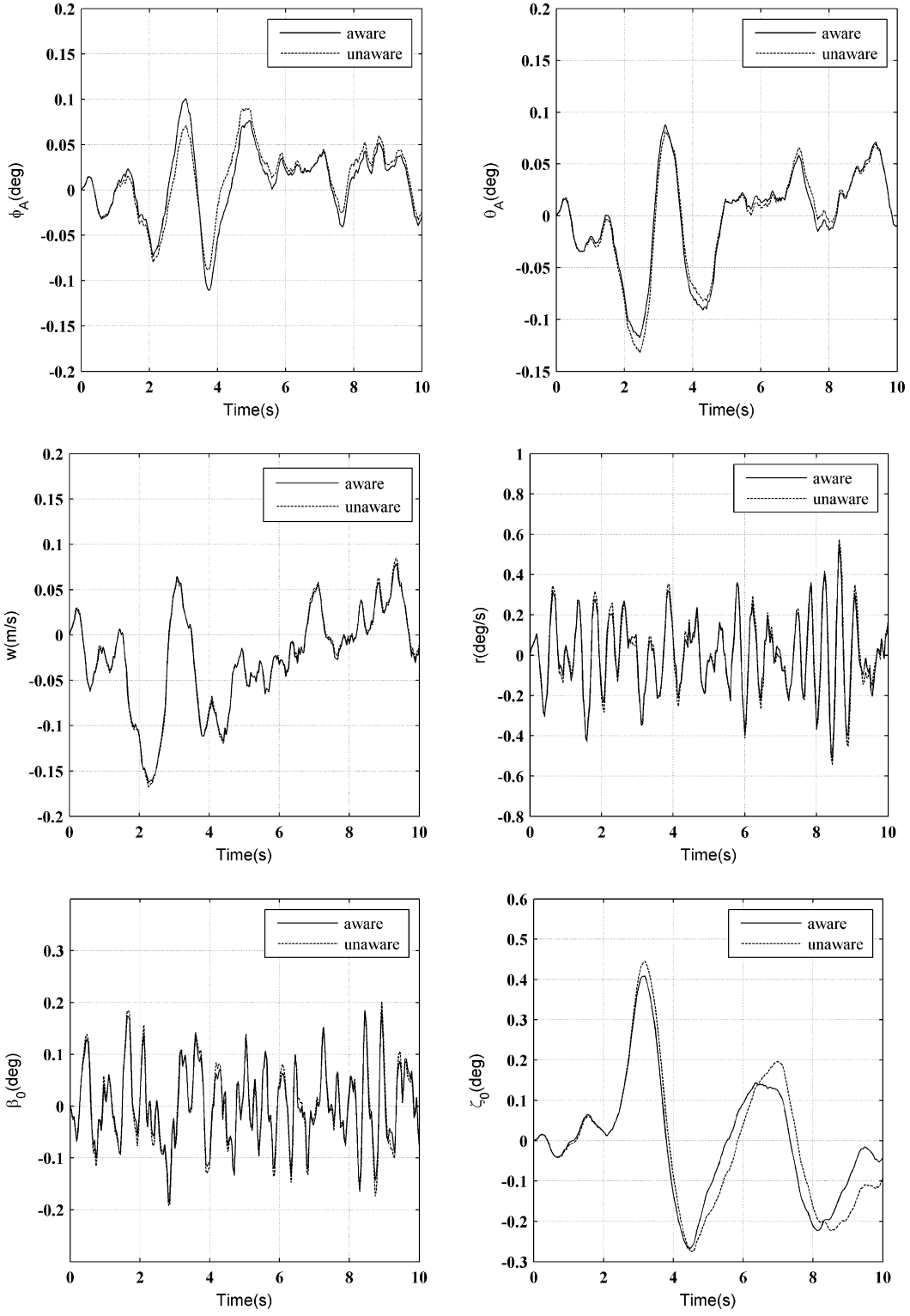

Fig. 9. Closed loop responses of some states using aware and unaware OVC for $M = 500$ kg.

variations with the mass comparable to the ones reported in Ref. [16] and these variations are in the same direction (e.g. the modes become more stable as the load mass increases). Also both load modes are exponentially stable in our model as well as in the one considered in Ref. [16]. In our model the frequency of the first load mode displays a variation with the mass which is not apparent in Ref. [16]. Third, the Phugoid mode is unstable while mass is changing, both in our studies and in Ref. [16]. One discrepancy we note here is that our Dutch Roll mode is unstable whereas in Ref. [16] it is reported as being exponentially stable. We remark, however, that the results reported in Ref. [16] were obtained for a different helicopter, namely UH-60, so differences between our results – for Puma SA 330 – and theirs are expected to occur. Moreover, our Dutch Roll mode compared perfectly well with results reported for Puma SA 330 in Ref. [36] (see Table 1).

Please cite this article in press as: T. Oktay, C. Sultan, Modeling and control of a helicopter slung-load system, Aerospace Science and Technology (2013), http://dx.doi.org/10.1016/j.ast.2013.03.005

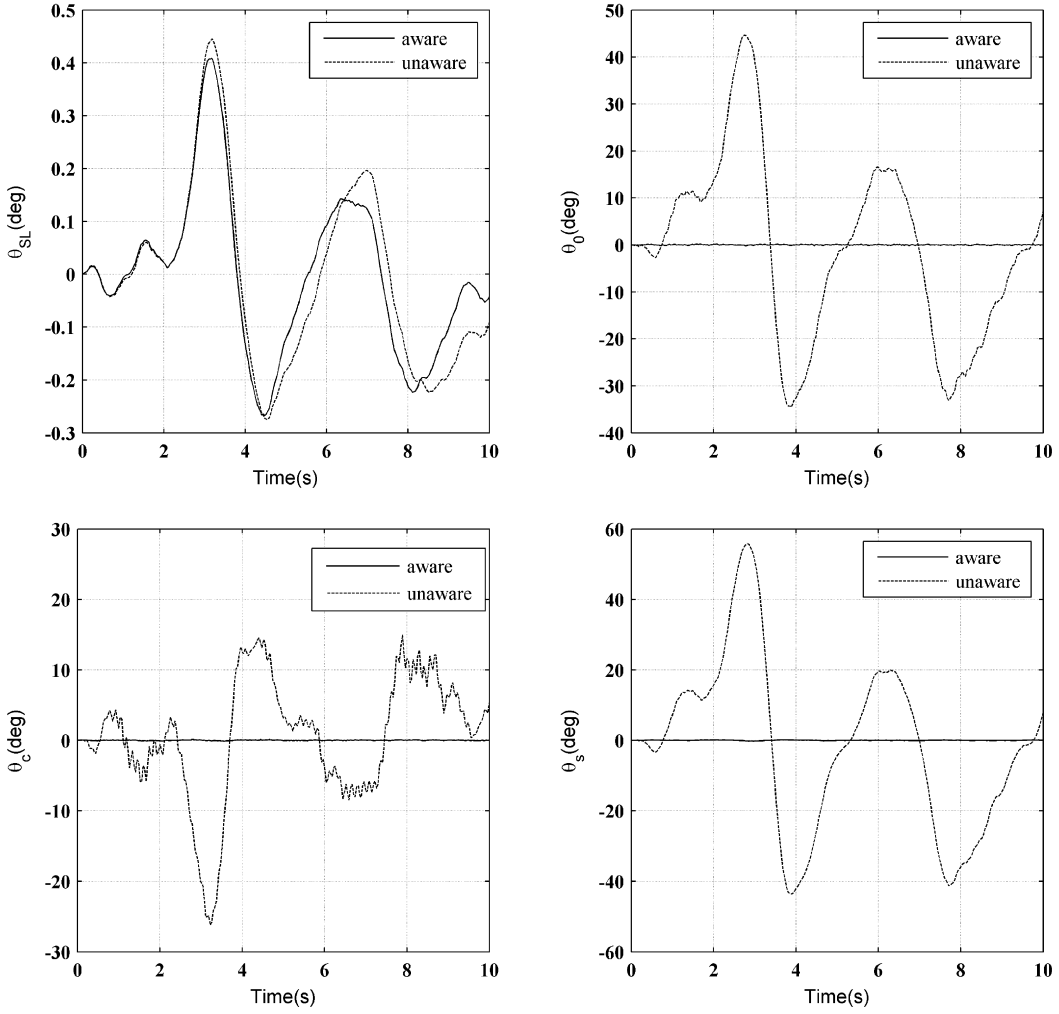

Fig. 10. Closed loop responses of some controls and longitudinal slung-load angle state using aware and unaware OVC for $M = 500$ kg.

We also studied the variation of the poles with the equivalent flat plat area, S. For this purpose we linearized the helicopter model around straight level flight. In Fig. 7 (left) we give the results obtained for $\mu = 0.2$, $M = 1000$ kg, $l = 5$ m. In Fig. 7 (right) we reproduce results from Ref. [16] obtained for the UH-60 helicopter and the same flight and load data: advance ratio of 0.2 and load mass of 1000 kg. We first notice that the load modes are exponentially stable with the first mode displaying a small variation with S compared to the second load mode. We also remark that the results agree qualitatively with those of Ref. [16] in the sense that all load modes are exponentially stable and their relative location in the complex plane as well as the relative size of the variations with S are similar with the ones ascertained by us (left of Fig. 7). The only minor discrepancy noted as far as the load modes are concerned is that the real part of the second load mode increases in our model with S, which is an opposite tendency to the one reported in Ref. [16]. Other discrepancies concern the Dutch Roll and Phugoid modes, which are unstable in our model. As noted in the previous paragraph, this is expected since we work with a different helicopter than Ref. [16]. Nevertheless, the variations of these flight dynamics modes with S are rather negligible and in the same direction as reported in Ref. [16].

Lastly, in Fig. 8 we also present results that address the variation of load modes and some helicopter modes with cable length, l, for a model linearized around hover and for $M = 500$ kg, $S = 0.4$ m^2. We first note that both load modes are exponentially stable, with the first load mode being more stable than the second (see Fig. 8 right, which reports data for UH-60). Also the frequency of the load modes decreases with increasing cable length, which is similar to the behavior reported in Ref. [16]. The Phugoid mode is unstable and displays a negligible variation when cable length changes, which also agrees with Ref. [16]. Like in the previous cases (i.e. Figs. 5 and 6), the discrepancy between the Dutch Roll modes, unstable in our model and exponentially stable in Ref. [16], persists due to the inherent differences between the two helicopters.

7. Control design and closed loop simulation results

A major issue in slung-load operations is the ability of the control system to maintain good performance and stability properties in the presence of uncertainties *and* the slung-load. Hence, for control design we consider as outputs of interest the Euler angles, i.e. we are interested in maintaining the attitude of the load carrying helicopter in the presence of measurement noise, model noise, and the slung-load. Guaranteeing that Euler angles variations are small is of the utmost importance for load carrying helicopters for a number of reasons that range from maintaining visual contact (e.g. for line of sight communication), to proper delivery of the load and landing. We also note that including control requirements (e.g. constraints) on the load itself is not expected to be effective because there is no direct control of the load, i.e. in the current

Please cite this article in press as: T. Oktay, C. Sultan, Modeling and control of a helicopter slung-load system, Aerospace Science and Technology (2013), http://dx.doi.org/10.1016/j.ast.2013.03.005

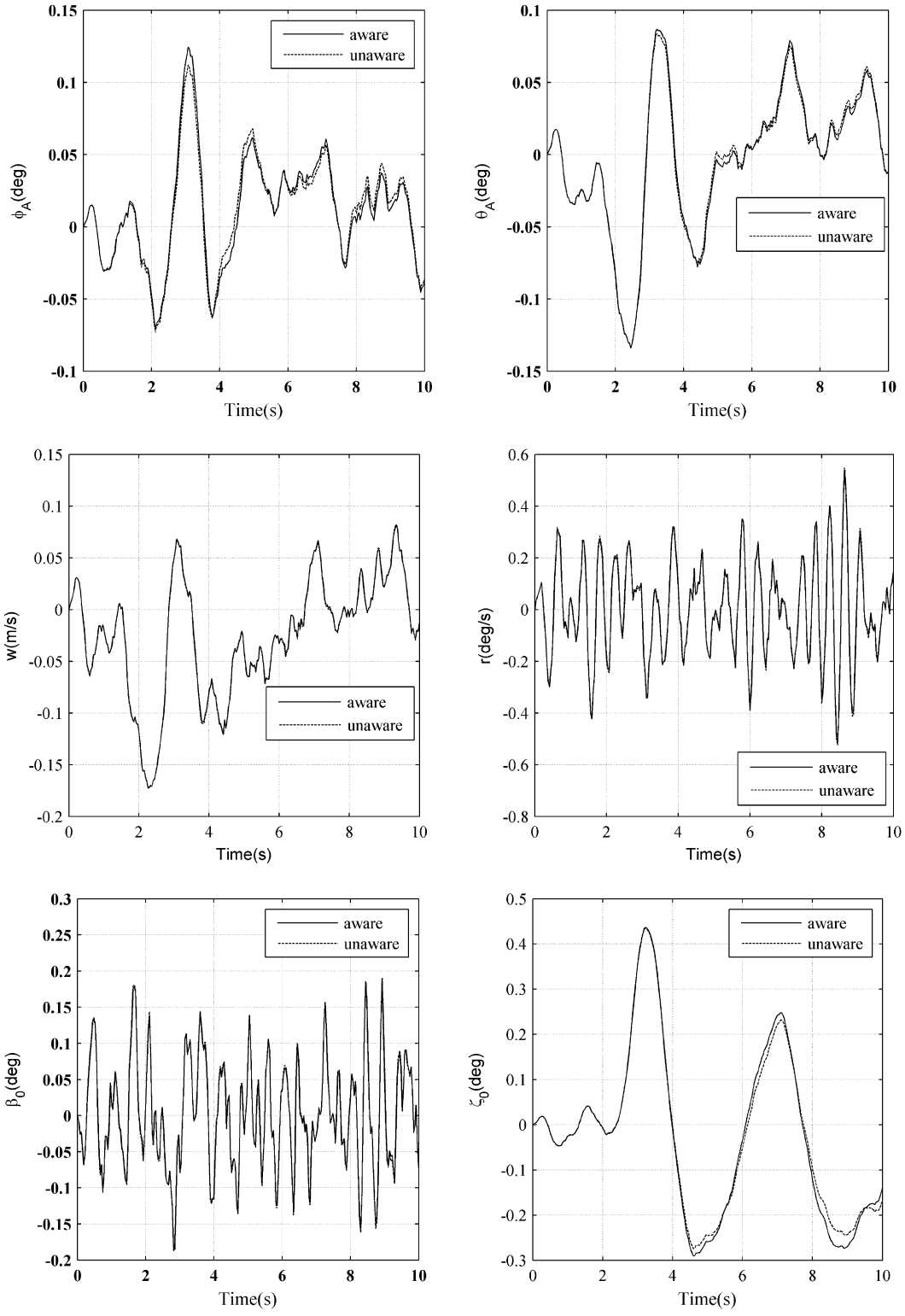

Fig. 11. Closed loop responses of some states using aware and unaware OVC for $M = 100$ kg.

scenarios the controls (also referred to as inputs) are all of the helicopter traditional controls, i.e. 3 main rotor controls and 1 tail rotor control. There is no physical control on the slung-load because the cable is a simple passive element.

For the first set of control design results presented next, the nonlinear helicopter slung-load model with $M = 500$ kg, $l = 5$ m, $S = 0.4$ m^2 was linearized around straight level flight at $V_A =$ 40 kts. Then the 1st OVC controller was designed for this linearized model with output variance constraint $\sigma^2 = 10^{-4}[\,1\ 1\ 0.1\,]$ on the helicopter Euler angles. The 1st IVC controller was also designed for this linearized model with input variance constraint $\mu^2 = 10^{-5}[\,1\ 1\ \ 1\,]$ on all helicopter controls. Next, we designed controllers for the unloaded (i.e. no slung-load carrying) helicopter as follows: the 2nd OVC and 2nd IVC controllers were designed

Please cite this article in press as: T. Oktay, C. Sultan, Modeling and control of a helicopter slung-load system, Aerospace Science and Technology (2013), http://dx.doi.org/10.1016/j.ast.2013.03.005

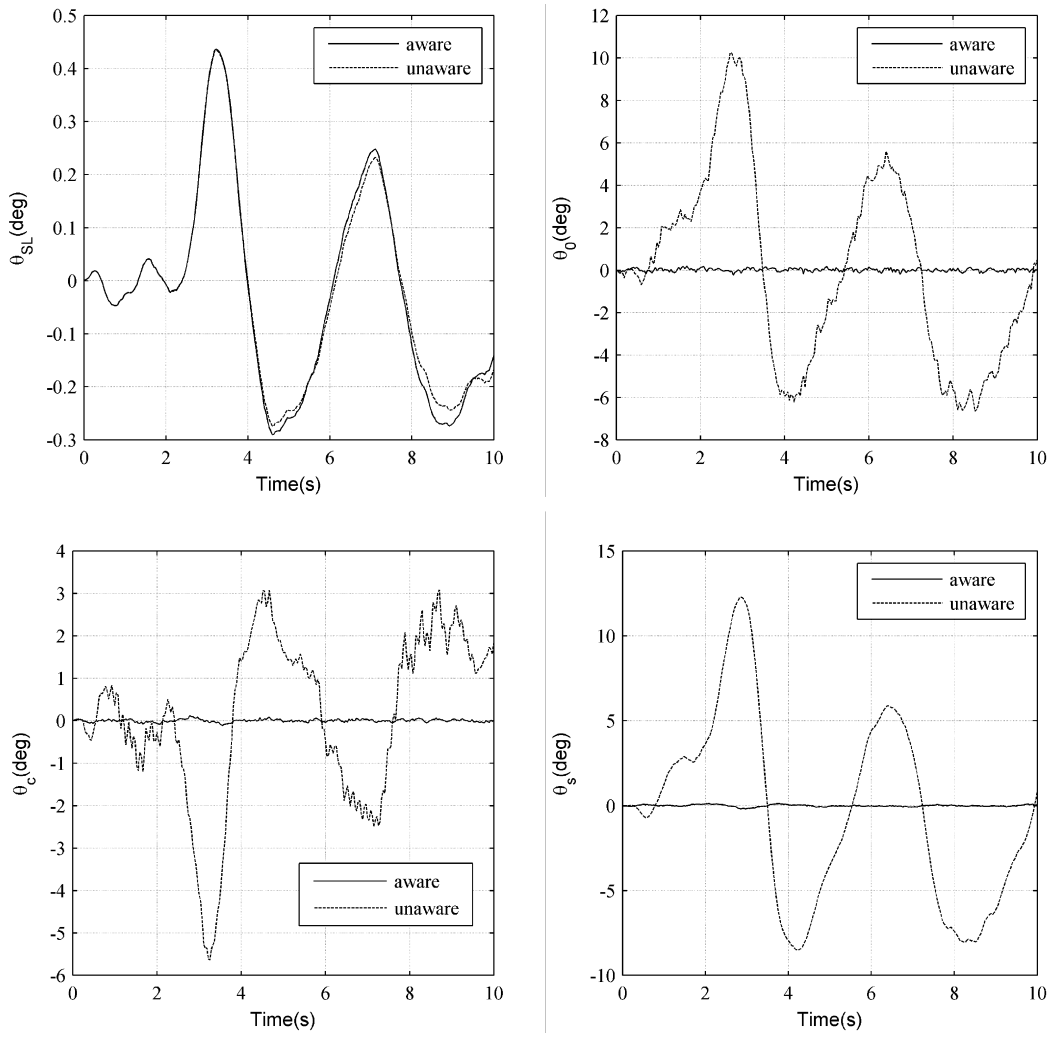

Fig. 12. Closed loop responses of some controls and longitudinal slung-load angle state using aware and unaware OVC for $M = 100$ kg.

for the linearized model of the unloaded helicopter at the same straight level flight condition (i.e. $V_A = 40$ kts) and considering the same variance constraints (i.e. $\sigma^2 = 10^{-4}[\,1\ 1\ 0.1\,]$ for OVC and $\mu^2 = 10^{-5}[\,1\ 1\ 1\ 1\,]$ for IVC). Since the 1st OVC and 1st IVC controllers were designed for the linearized model of the helicopter slung-load system, they were named "aware" controllers. Similarly, because the 2nd OVC and 2nd IVC controllers were designed for the linearized model of the unloaded helicopter, they were called "unaware" controllers. These denominations need some explanation. The unaware controllers are controllers that have been designed for the unloaded helicopter *only*. They have a fixed architecture and once implemented they cannot be modified to accommodate for configuration changes or the addition of a load. On the other hand, the "aware" controllers are specifically designed for load carrying missions, hence they are indeed "aware" of the load. Switching between aware and unaware controllers can be performed however, for practical implementation this requires additional equipment (e.g. a supervisory control) which might not be available. Therefore, the study of "unaware" controllers in the presence of a slung-load is very valuable because it indicates the expected performance that can be obtained only with these controllers.

Note that for the numerical experiments reported in this article, the sensor measurements were helicopter linear velocities, angular velocities and Euler angles, and the nondimensionalized noise intensities were $W = 10^{-7} I_{29}$, $V = 10^{-7} I_9$. In general V depends on sensor quality (high quality sensors correspond to small V) whereas W is dictated by the quality of the modeling process. These intensities are apparently small for two reasons. Firstly, these are in fact nondimensionalized values. To get dimensional values some of the components of W must be multiplied by large numbers (i.e. for the linear velocities a factor of 202.5 m/s and for the angular velocities a factor of 27 rad/s are necessary for Puma SA 330). Secondly, because of the sophisticated modeling, which accounts for many physical effects, the models are considered sufficiently accurate (see [26] for larger noise intensities on no slung-load carrying helicopters). The states and controls are in nondimensional form for computations, but they are dimensionalized in the simulation figures. Also note that all states and controls given in the figures are variations from the nominal values, as it is typically the case when linearization is used.

7.1. OVC results

OVC control design was pursued using the data and scenarios described in the previous paragraphs. Convergence of the gain selection algorithm used to design OVC controllers was fast (e.g. 8 iterations for the 1st OVC controller) despite of the fact that the systems are large (e.g. matrix A_p size is 29×29).

After control design we evaluated closed loop systems performance. For this purpose we created the 1st closed loop system by integrating the linearized helicopter slung-load system and the

Please cite this article in press as: T. Oktay, C. Sultan, Modeling and control of a helicopter slung-load system, Aerospace Science and Technology (2013), http://dx.doi.org/10.1016/j.ast.2013.03.005

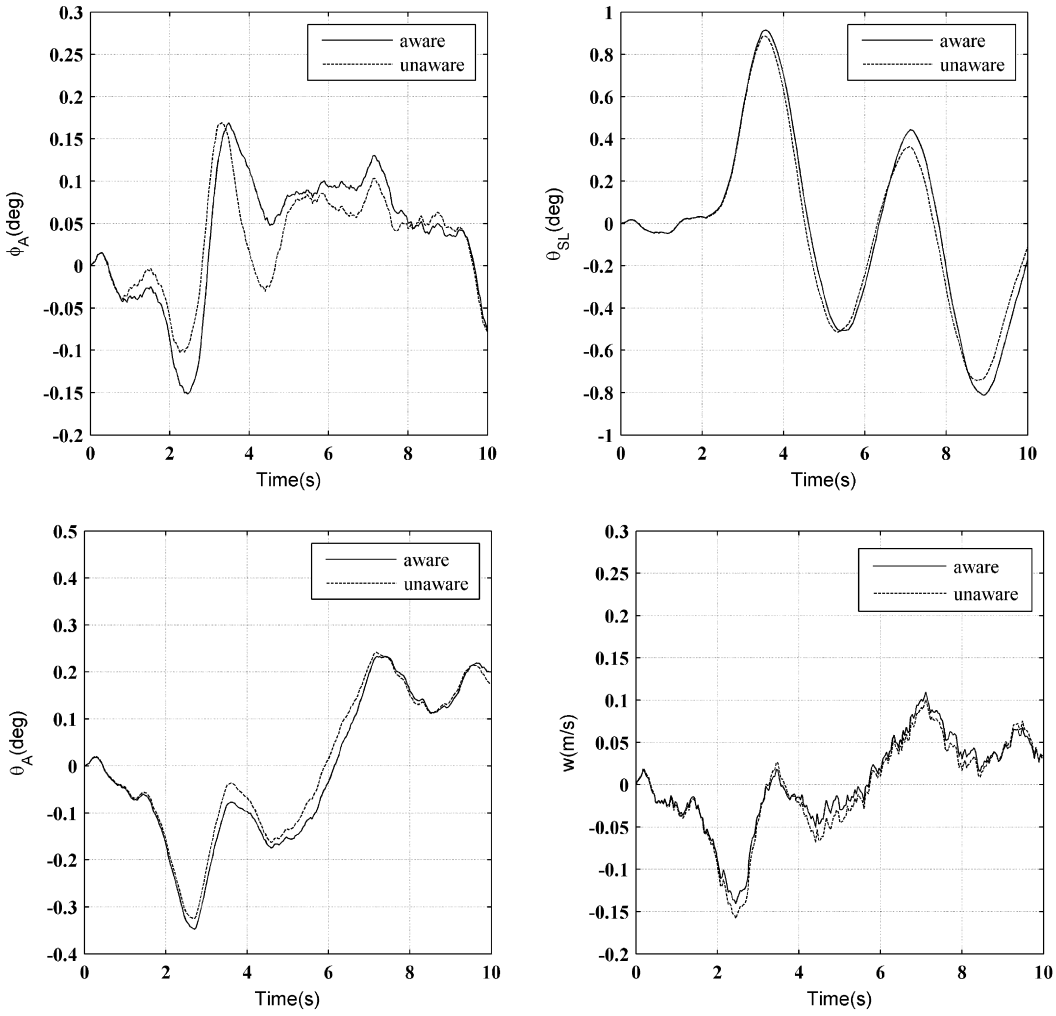

Fig. 13. Closed loop responses of some states using IVC for $M = 500$ kg.

aware OVC controller. This controller is expected to perform very well in the ideal operational condition when the helicopter carries a load. The 2nd closed loop system was created by integrating the linearized helicopter slung-load system and unaware OVC controller. This second scenario corresponds to the situation when the helicopter is not equipped with an additional supervisory control to determine that switching between controllers (i.e. to the aware OVC controller) is necessary when load is added to the helicopter. It is also a very likely situation to occur when a helicopter which is not normally tasked to carry loads is required (e.g. due to an emergency situation) to perform such a mission. In Fig. 9 closed loop responses of selected helicopter states (i.e. ϕ_A, θ_A, w, r, β_0, ζ_0) and in Fig. 10 closed loop responses of selected controls (i.e. θ_0, θ_c, θ_s) and longitudinal slung-load angle state (i.e. θ_{SL}) are given for both aware and unaware controllers. For the closed loop simulations both systems were excited using white noise perturbations of nondimensionalized intensities $W = 10^{-7} I_{29}, V = 10^{-7} I_9$.

The first observation is that these controllers are both exponentially stabilizing the corresponding closed loop systems. This is guaranteed by the OVC theory [40,41] for the first closed loop system, whereas for the second it indicates that the unaware OVC controller has good stability robustness properties with respect to modeling uncertainties introduced by the load. Note that exponential stability of the 2nd closed loop was ascertained by computing the poles of the linear closed loop system, which were all located in the left hand side of the complex plane. Second, from Figs. 8 and 9 we see that the responses of ϕ_A, θ_A, w, r, β_0, ζ_0, θ_{SL} obtained when the aware OVC controller was used are within small, expected limits, and do not display dangerous behavior. Our extensive numerical experiments showed that these conclusions are valid for all states. Closed loop responses of some other states (i.e. u, v, p, q, β_c, β_s, ζ_c, ζ_s) are given in Figs. A.1 and A.2 in Appendix A. For the Euler angle states this is expected because the aware OVC controller was specifically designed to minimize the variances of these outputs. Fig. 10 also shows that this good behavior is achieved by the aware OVC controller with very small control variations, which is a reflection of the fact that this controller minimizes control energy.

When analyzing the performance of the unaware OVC controller, we note from Fig. 9 that the responses of ϕ_A, θ_A, w, r, β_0, ζ_0, θ_{SL} are similar to the ones found using the aware OVC controller. However, Fig. 10 shows that this comes at an unreasonable price: the responses of θ_0, θ_c, θ_s when the unaware controller is used are much larger than the ones obtained using the aware controller. Actually these variations are so large that even the small angles assumption used in linearization is violated. These results, which are expected because the unaware controller was not designed for the load carrying scenario, clearly advocate for the addition of a supervisory control system to switch between controllers when load is added to/discarded from the helicopter. Controllers for slung-load carrying helicopters could be, for example, imple-

Please cite this article in press as: T. Oktay, C. Sultan, Modeling and control of a helicopter slung-load system, Aerospace Science and Technology (2013), http://dx.doi.org/10.1016/j.ast.2013.03.005

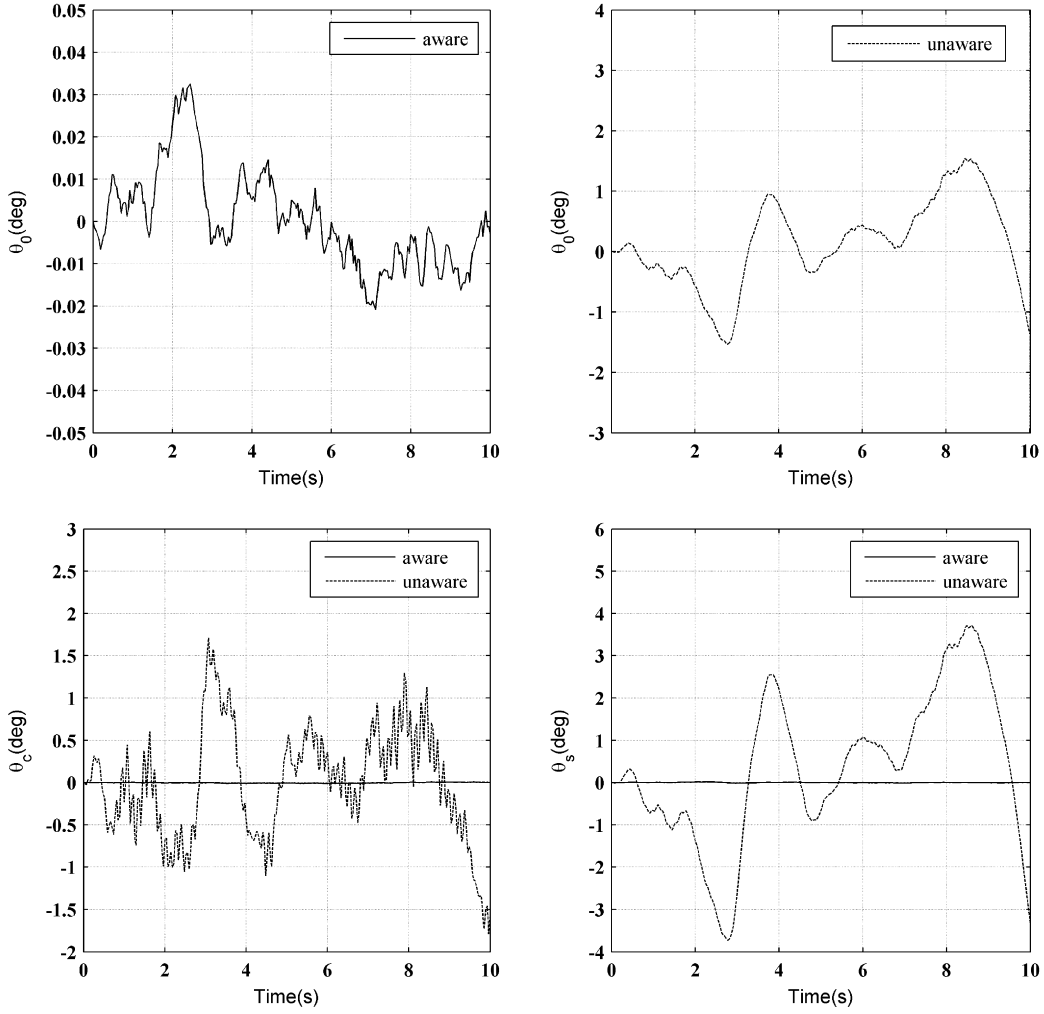

Fig. 14. Closed loop responses of some controls using IVC for $M = 500$ kg.

mented as gain scheduled controllers where the key parameter that governs the scheduling process is the slung-load mass.

In order to confirm the results illustrated in Figs. 8–9, we repeated the linearization and control design process for other flight conditions, specifically, hover and straight level flight at 80 kts. We then created closed loop systems using aware and unaware controllers and simulated their responses to white noise excitations. These simulations are not reproduced here for brevity, however at the end of this process we reached conclusions similar to the ones obtained for straight level flight at 40 kts: the controllers are exponentially stabilizing the corresponding closed loop systems, displaying good stability robustness, but the unaware controllers have to work much harder to accommodate heavy loads.

Note that unaware OVC controllers can still be used for smaller loads. For example Figs. 11–12 show that the counterparts of Figs. 9–10 for $M = 100$ kg. Clearly, the unaware OVC controller is capable of safely handling this load with tolerable control variations.

7.2. IVC results

To complete the study of variance controllers on helicopter slung-load systems we repeated the analysis carried out in Section 7.1 for IVC control design. For this purpose we created the 1st and 2nd closed loop systems in a similar way with the ones used in OVC studies, i.e. using aware and unaware IVC controllers, respectively. We then simulated closed loop responses when the systems are subject to the same white noise perturbations like their counterparts in the closed loop OVC control analysis. In Fig. 13 closed loop responses of selected states (i.e. ϕ_A, θ_A, w, θ_{SL}) and in Fig. 14 closed loop responses of selected controls (i.e. θ_0, θ_c, θ_s) are given for both aware and unaware IVC controllers.

Similarly with the OVC case, both closed loop systems obtained using IVC controllers are exponentially stable. Therefore, the unaware IVC controller displays good stability robustness with respect to load addition, similarly with OVC unaware controllers. Fig. 13 shows that the responses of ϕ_A, θ_{SL} obtained using the aware IVC controller are similar to the ones found using the unaware IVC controller. However, we remark from Fig. 14 that this time, even though the responses of θ_0, θ_c, θ_s obtained using the unaware IVC controller are larger than the ones obtained using the aware IVC controller, they do not exhibit unreasonably large variations like in the unaware OVC case (i.e. Fig. 10). This fact can be explained by the nature of IVC control design, which explicitly imposes constraints on the variance of *each* control input, unlike OVC control design.

Extensive numerical experiments indicate that these conclusions are suitable for all states and all controls. In Figs. A.3 and A.4 responses of some other states (i.e. u, v, p, q, β_c, β_s, ζ_c, ζ_s) are given (see Appendix A). All these conclusions drawn in this

Please cite this article in press as: T. Oktay, C. Sultan, Modeling and control of a helicopter slung-load system, Aerospace Science and Technology (2013), http://dx.doi.org/10.1016/j.ast.2013.03.005

subsection are also valid for other flight conditions (e.g. hover and 80 kts).

B. Conclusions

A control oriented, physics based helicopter and slung-load model was developed. The helicopter model includes blade flapping and lead-lagging dynamics while for the slung-load a point mass model was used. A quasi-steady aerodynamic drag force acting on the slung load was modeled in the direction of the local airflow. The resulting nonlinear equations of motion of the helicopter slung-load system were trimmed and linearized around different straight level flight conditions. The behaviors of the resulting trims (i.e. cable angle, longitudinal and lateral cyclic pitch angles) and modes (i.e. load modes, Phugoid mode, and Dutch roll mode) as functions of some parameters (i.e. cable length, load mass, equivalent flat plate area, and flight speed) were thoroughly analyzed. These studies resulted in modes and trim values that are in the range reported in the literature. Discrepancies between these behaviors and those reported in the literature can be explained primarily by the differences between helicopter types.

Linearized models were used for the design of output variance constrained (OVC) and input variance constrained (IVC) controllers. These controllers were designed both for linearized models of unloaded helicopters, and called "unaware" (i.e. of the load) controllers, and for linearized models of slung-load carrying helicopters, and called "aware" controllers. Closed loop system responses of selected states and controls were given and these controllers performance was examined. All variance constrained controllers studied (aware as well as unaware) exponentially stabilized the nominal flight conditions. Behaviors of closed loop system states using aware variance constrained controllers are close to the ones obtained using unaware controllers. However, the aware controllers showed much better performance than unaware ones in terms of control responses. Specifically, the unaware controllers displayed larger variations for the controls than the aware controllers. Increasing control inputs raises control cost and may cause failure of operation.

Therefore, using aware variance constrained controllers during slung-load operations is advantageous both for energy efficiency and safety. This requires switching between controllers when load is added to/discarded from the helicopter. Since switching can nowadays be reliably implemented due to recent advances in control technology, signals processing, microelectronics, power electronics, and microprocessors, using aware variance constrained controllers is highly advised.

Appendix A

This appendix contains additional OVC results (see Figs. A.1, A.2), additional IVC results (see Figs. A.3, A.4) and key helicopter parameters (see Table A.1),

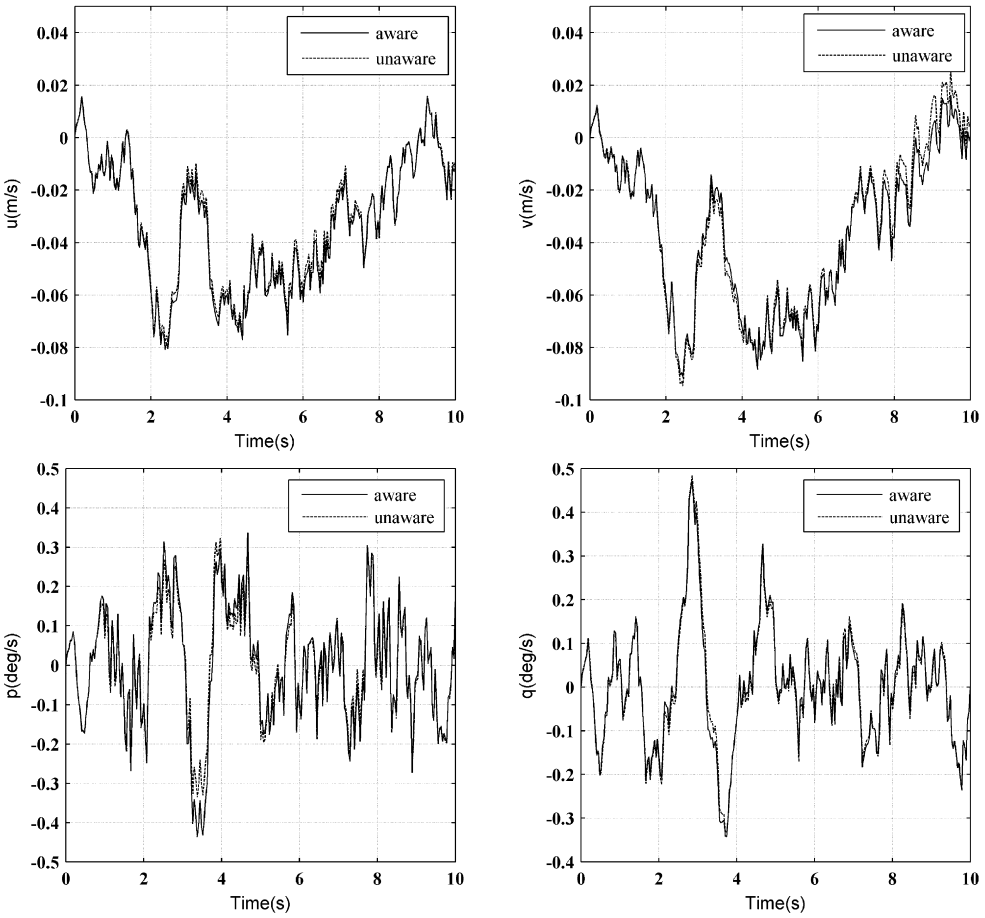

Fig. A.1. Closed loop responses of additional fuselage states using OVC for $M = 500$ kg.

Please cite this article in press as: T. Oktay, C. Sultan, Modeling and control of a helicopter slung-load system, Aerospace Science and Technology (2013), http://dx.doi.org/10.1016/j.ast.2013.03.005

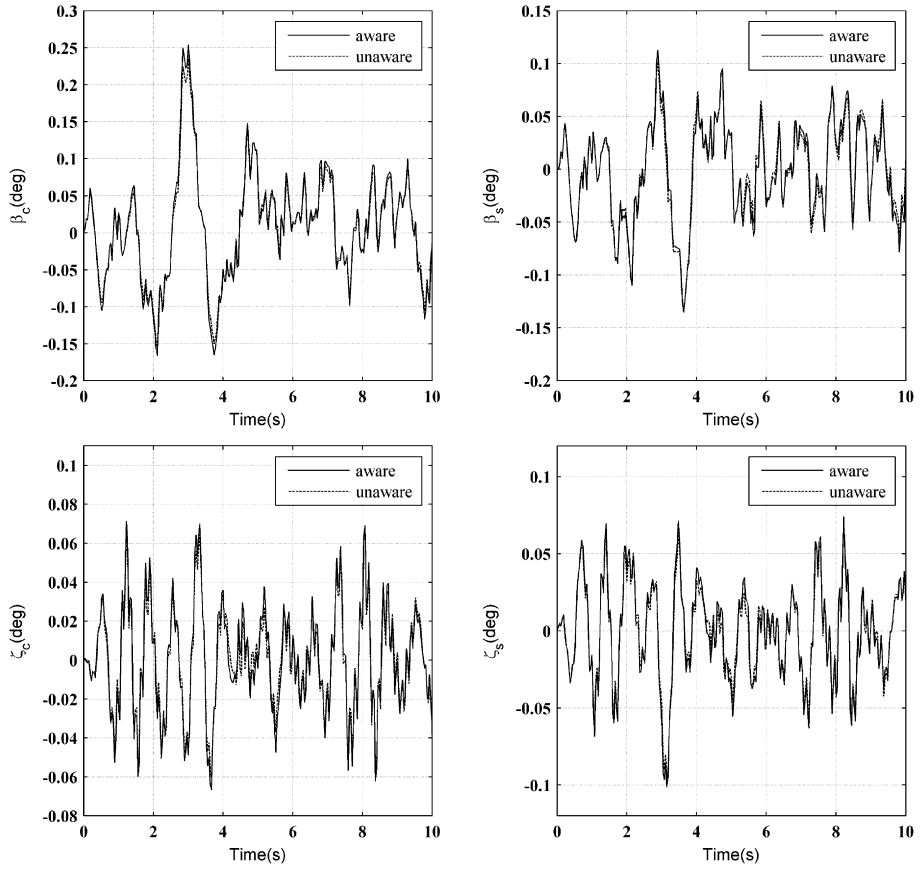

Fig. A.2. Closed loop responses of additional blade states using OVC for $M = 500$ kg.

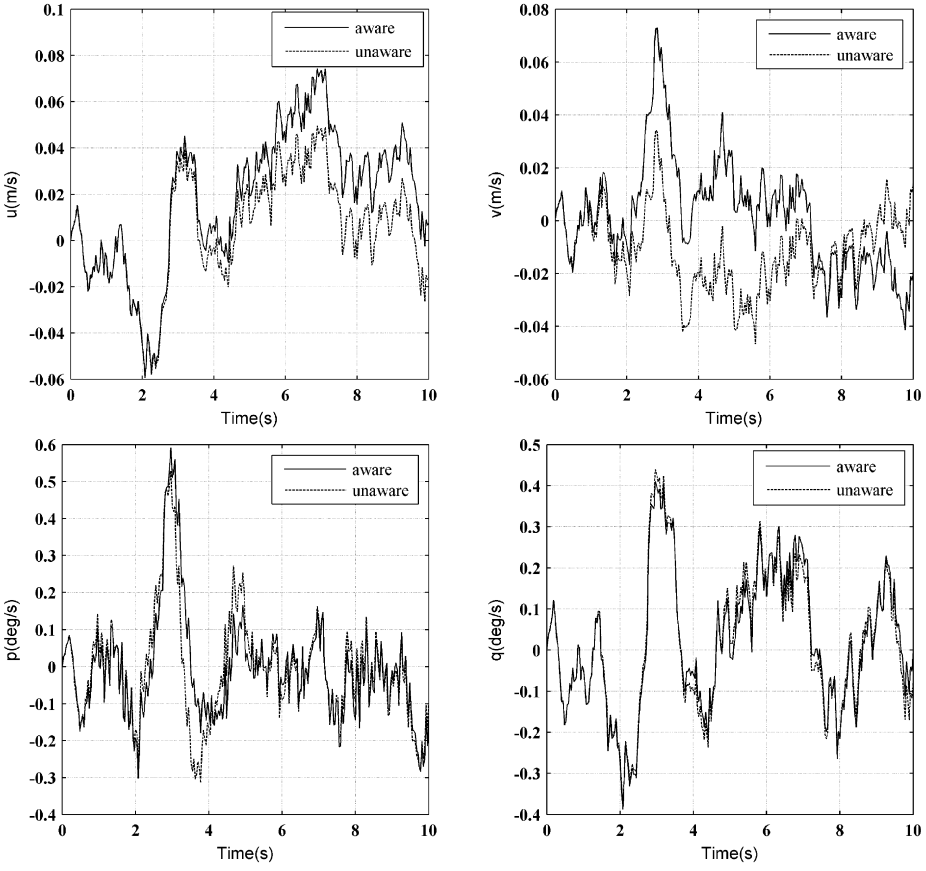

Fig. A.3. Closed loop responses of additional fuselage states using IVC for $M = 500$ kg.

Please cite this article in press as: T. Oktay, C. Sultan, Modeling and control of a helicopter slung-load system, Aerospace Science and Technology (2013), http://dx.doi.org/10.1016/j.ast.2013.03.005

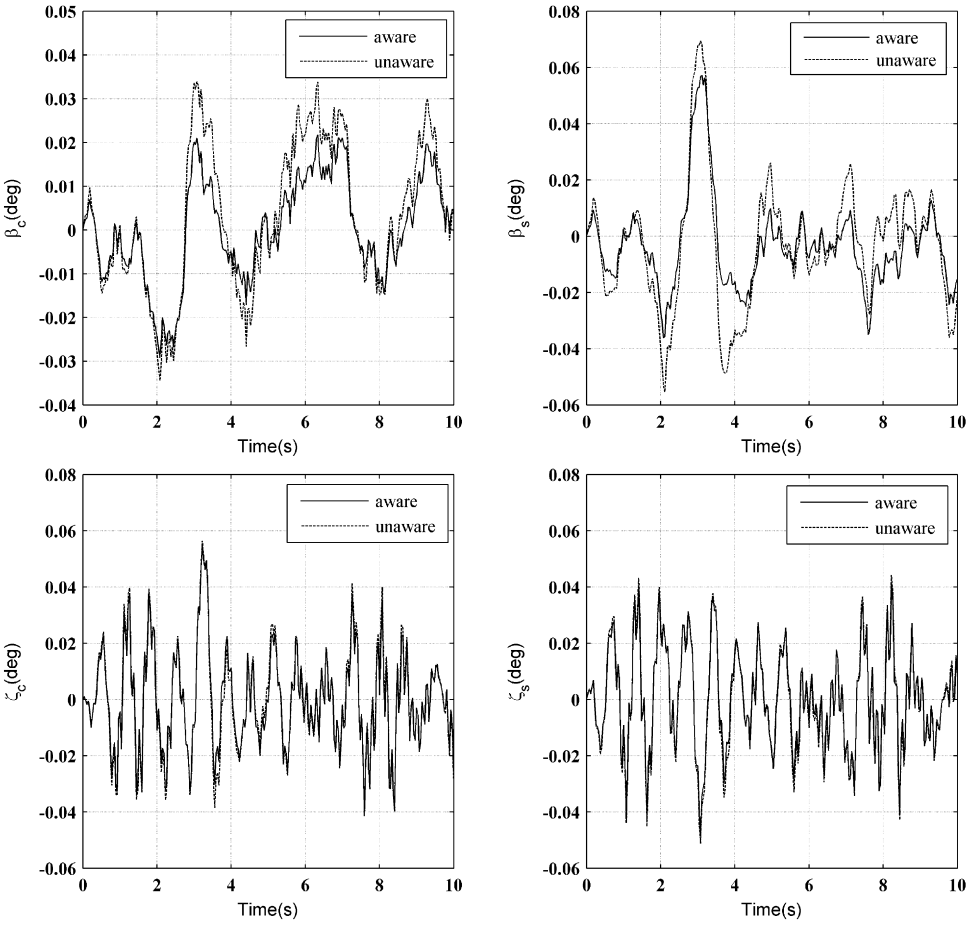

Fig. A.4. Closed loop responses of additional blade states using IVC for $M = 500$ kg.

Table A.1
Important configuration data of Puma SA 330.

Quantity	Symbol	Magnitude	Reference
Moments of inertia	I_{xx}	9638 kg m^2	[36]
	I_{yy}	33 240 kg m^2	
	I_{zz}	25 889 kg m^2	
	I_{xz}	2226 kg m^2	
Number of blades	N_b	4	[36]
Rotor radius	R	7.5 m	[36]
Hinge offset	e	0.285 m	[36]
Main rotor angular velocity	Ω	27 rad/s	[36]
Helicopter mass	M_a	5805 kg	[36]
Flapping spring stiffness coefficient	K_β	48 149 N m/rad	[36]
Lagging spring stiffness coefficient	K_ζ	100 000 N m/rad	[36]*
Lagging damper damping coefficient	C_ζ	10 000 N m s/rad	[36]*
Blade inertia	I_b	1280 kg m^2	[36]
Blade twist	θ_{tw}	−0.14 rad	[36]
Blade profile drag	δ_0	0.01	[11]
Blade induced drag	δ_2	0.4	[11]
Blade lift coefficient	a	5.73/rad	[36]
Vertical distance helicopter's center of gravity (cg) to hub	h	2.157 m	[36]*
Vertical distance cg to tail rotor	z_T	1.585 m	[36]
Horizontal distance cg to tail rotor	x_T	9 m	[36]
Tail rotor thrust coefficient	K_T	8000 N/rad	*
Vertical distance cg to nose	z_F	0.55 m	[36]*
Horizontal distance cg to nose	x_F	3.80 m	[36]*
Fuselage skin friction coefficient	c_{d_f}	0.02	[18]*
Fuselage pressure drag coefficient	c_{d_p}	1.2	[18]*
Fuselage length	l	14 m	[36]*
Fuselage diameter	d	3 m	[36]*
Lock number	γ	9.374	[36]

* Estimated parameter using available data.

Please cite this article in press as: T. Oktay, C. Sultan, Modeling and control of a helicopter slung-load system, Aerospace Science and Technology (2013), http://dx.doi.org/10.1016/j.ast.2013.03.005

References

[1] E. Altug, J.P. Ostrowski, R. Mahony, Control of a quadrotor helicopter using visual feedback, in: Proceedings of the IEEE International Conference on Robotics and Automation, Washington, DC, 2002.
[2] P. Apkarian, C. Champetier, J.F. Magni, Design of a helicopter output feedback control law using modal and structured-robustness techniques, International Journal of Control 50 (4) (1989) 1195–1215.
[3] M. Bisgaard, A.C. Harbo, J.D. Bendsten, Full state estimation for helicopter slung load system, in: AIAA Guidance, Navigation, and Control Conference, Hilton Head, SC, 2007.
[4] M. Bisgaard, A.C. Harbo, J.D. Bendtsen, Adaptive control system for autonomous helicopter slung load operations, Control Engineering Practice 18 (7) (2010) 800–811.
[5] L.Y. Bo, L.W. Zhu, S. Qi, Improved LQG control for small unmanned helicopter based on active model in uncertain environment, in: International Conference on Electronics, Communications and Control (ICECC), Ningbo, China, 2011.
[6] L.S. Cicolani, et al., Flight-time identification of a UH-60A helicopter and slung load, NASA TM-112231, 1998.
[7] L.S. Cicolani, A. Cone, Theron, N. Johannes, D. Robinson, J. Lusardi, M.B. Tischler, A. Rosen, R. Raz, Flight test and simulation of a cargo container slung load in forward flight, Journal of American Helicopter Society 54 (3) (2009) 32006-1-32006-18(18).
[8] L.S. Cicolani, G. Kanning, Equations of motion of slung-load systems, including multilift systems, NASA TN 3280, 1992.
[9] L.S. Cicolani, R. Raz, A. Rosen, N.J. Theoren, J. Lusardi, M.B. Tischler, D. Robinson, Flight test, simulation and passive stabilization of a cargo container slung load in forward flight, in: American Helicopter Society 63rd Annual Forum, Virginia Beach, VA, USA, 2007.
[10] E.M. Cliff, D.B. Bailey, Dynamic stability of a translating vehicle with a simple sling load, Journal of Aircraft 12 (10) (1975).
[11] M.E. Dreier, Introduction to helicopter and tiltrotor flight simulation, in: AIAA Education Series, 2007, pp. 133–137, 591.
[12] T.A. Dukes, Maneuvering heavy sling loads near hover, Part I: Damping the pendulous motion, Journal of the American Helicopter Society 18 (2) (1973).
[13] T.A. Dukes, Maneuvering heavy sling loads near hover, Part II: Some elementary maneuvers, Journal of the American Helicopter Society 18 (3) (1973).
[14] E.P.N. Duque, R. Gordon, M.D. Berry, L. Cicolani, A. Rosen, Reynolds-averaged Navier–Stokes simulations of helicopter slung-loads, in: American Helicopter Society 4th Decennial Specialist's Conference on Aeromechanics, San Francisco, CA, USA, 2004.
[15] D. Fusato, R. Celi, Multidisciplinary design optimization for helicopter aeromechanics and handling qualities, AIAA Journal of Aircraft 43 (1) (2006) 241–252.
[16] D. Fusato, G. Guglieri, R. Celi, Flight dynamics of an articulated rotor helicopter with an external slung load, Journal of the American Helicopter Society 46 (1) (2001) 3–14.
[17] A.C. Harbo, M. Bisgaard, State-control trajectory generation for helicopter slung load system using optimal control, in: AIAA Guidance, Navigation, and Control Conference, Chicago, IL, 2009.
[18] S.F. Hoerner, Fluid dynamic drag, in: Hoerner Fluid Dynamics, 1965, pp. 2.1 3.9.
[19] C. Hsieh, R.E. Skelton, F.M. Damra, Minimum energy controllers with inequality constraints on output variances, Optimal Control Application and Methods 10 (4) (1989) 347–366.
[20] C.Y. Huang, R. Celi, I.C. Shih, Reconfigurable flight control systems for a tandem rotor helicopter, Journal of the American Helicopter Society 44 (1) (1999) 50–62.
[21] C.M. Ivler, M.B. Tischler, J.D. Powell, Cable angle feedback control systems to improve handling qualities for helicopters with slung loads, in: Proceedings of the AIAA Guidance, Navigation, and Control Conference, Portland, OR, 2011.
[22] Z. Jiang, J. Han, Y. Wang, Q. Song, Enhanced LQR control for unmanned helicopter in hover, in: 1st International Symposium on Systems and Control in Aerospace and Astronautics, Harbin, China, 2006.
[23] R. Kureemun, D.J. Walker, B. Manimala, M. Voskuijl, Helicopter flight control law design using H_∞ techniques, in: Proceedings of the 44th IEEE Conference on Decision and Control, and the European Control Conference, Seville, Spain, 2005.
[24] L.R. Lucassen, F.J. Sterk, Dynamic stability analysis of a hovering helicopter with a sling load, Journal of the American Helicopter Society 10 (2) (1965).
[25] C.C. Luo, R.F. Liu, Y.H. Chang, Helicopter H_∞ control design with robust flying quality, Aerospace Science and Technology 7 (2003) 159–169.
[26] T. Oktay, Constrained control of complex helicopter models, Ph.D. Dissertation, Virginia Tech, May 2012.
[27] T. Oktay, C. Sultan, Variance constrained control of maneuvering helicopters with sensor failure, Proceeding of the Mechanical Engineers, Part G, Journal of Aerospace Engineering (2012), http://dx.doi.org/10.1177/0954410012464002.
[28] T. Oktay, C. Sultan, Constrained predictive control of helicopters, Journal of Aircraft Engineering and Aerospace Technology 85 (1) (2013) 32–47.
[29] T. Oktay, C. Sultan, Simultaneous helicopter and control system design, Journal of Aircraft (2013), in press, http://dx.doi.org/10.2514/1.C032043.
[30] T. Oktay, C. Sultan, Control energy reduction via helicopter rotor active morphing, Journal of Aircraft, submitted for publication.
[31] T. Oktay, C. Sultan, Variance constrained control of maneuvering helicopters, in: Proceedings of American Helicopter Society 68th Annual Forum, Forthworth, TX, USA, 2012.
[32] T. Oktay, C. Sultan, Model predictive control of maneuvering helicopters, in: Proceedings of AIAA Guidance, Navigation and Control Conference, Minneapolis, MN, USA, 2012.
[33] T. Oktay, C. Sultan, Integrated maneuvering helicopter model and controller design, in: Proceedings of AIAA Guidance, Navigation and Control Conference, Minneapolis, MN, USA, 2012.
[34] T. Oktay, C. Sultan, Robustness of variance constrained controllers for complex, control-oriented helicopter models, in: Proceedings of American Control Conference, Washington, DC, WA, USA, 2013.
[35] H.M. Omar, New fuzzy-based anti-swing controller for helicopter slung-load system near hover, in: IEEE International Symposium on Computational Intelligence in Robotics and Automation, Daejeon, Korea, 2009.
[36] G.D. Padfield, Helicopter flight dynamics, in: AIAA Education Series, 2007, pp. 282–287.
[37] C. Poli, D. Cromack, Dynamics of slung bodies using a single-point suspension system, Journal of Aircraft 10 (2) (1973).
[38] K.R. Reddy, T.T. Stuckey, K.J. Bourne, Dynamic simulation of a helicopter carrying a slung load, in: International Congress on Modeling and Simulation Proceedings, Christchurch, New Zealand, 2007.
[39] V. Sahasrabudhe, M. Tischler, R. Cheng, A. Stumm, M. Lavin, Balancing CH-53K handling qualities and stability margin requirements in the presence of heavy external loads, in: American Helicopter Society 63rd Forum, Virginia Beach, VA, May 2007.
[40] R.E. Skelton, Dynamic Systems Control: Linear Systems Analysis and Synthesis, John Wiley & Sons, 1987, Chapter 8.
[41] R.E. Skelton, T. Iwasaki, K. Grigoriadis, A Unified Algebraic Approach to Linear Control Design, Taylor & Francis, 1998, Chapter 4.
[42] R.E. Skelton, M.D. Lorenzo, Space structure control design by variance assignment, Journal of Guidance, Control, and Dynamics 8 (4) (1985) 454–462.
[43] R.A. Stuckey, Mathematical modeling of helicopter slung-load systems, DSTO Technical Report DSTO-TR-1257, Melbourne, Australia, 2001, p. 42.
[44] K. Thanapalan, T.M. Wong, Modeling of a helicopter with an under-slung load system, in: Proceedings of the 29th Chinese Control Conference, Beijing, China, 2010.
[45] N.J. Theoren, R. Gordon, L. Cicolani, A. Rosen, E.P.N. Duque, R.H. Hasley, Computational fluid dynamics calculation of a helicopter slung load, in: AIAA 36th Fluid Dynamics Conference, San Francisco, CA, USA, 2006.
[46] R. Xie, X. Wang, Y. Li, H_∞ State feedback control for the stabilization of the three Euler angles of helicopter based on LMI, in: International Conference on Intelligent Computation Technology and Automation, Hunan, China, 2008.
[47] W.M. Zhang, Hovering control and simulation of a tandem helicopter using LQR approach, Microcomputer Information 26 (9–1) (2010).
[48] G. Zhu, M.A. Rotea, R.E. Skelton, A convergent algorithm for the output covariance constraint control problem, SIAM Journal on Control and Optimization 35 (1) (1997) 341–361.
[49] G. Zhu, R.E. Skelton, Mixed L_2 and L_∞ problems by weight selection in quadratic optimal control, International Journal of Quadratic Optimal Control 63 (5) (1991) 1161–1176.

Please cite this article in press as: T. Oktay, C. Sultan, Modeling and control of a helicopter slung-load system, Aerospace Science and Technology (2013), http://dx.doi.org/10.1016/j.ast.2013.03.005